Progress In Electromagnetics Research Letters, Vol. 22, 165–174, 2011

EFFECTIVE PERMITTIVITY TENSOR FOR A METAL-DIELECTRIC SUPERLATTICE

B. Zenteno-Mateo, V. Cerdán-Ramírez and B. Flores-Desirena

Facultad de Ciencias Físico-Matemáticas
Benemérita Universidad Autónoma de Puebla
Apdo. Post. 1152, Puebla, Pue. 72000, Mexico

M. P. Sampedro

Facultad de Ingeniería Química
Benemérita Universidad Autónoma de Puebla
C.U., Puebla, Pue. 72570, Mexico

E. Juárez-Ruiz

Facultad de Ciencias de la Electrónica
Benemérita Universidad Autónoma de Puebla
C.U., Puebla, Pue. 72570, Mexico

F. Pérez-Rodríguez

Instituto de Física
Benemérita Universidad Autónoma de Puebla
Apdo. Post. J-48, Puebla, Pue. 72570, Mexico

Abstract—We have derived simple analytical expressions for the frequency-dependent effective permittivity tensor of a one-dimensional metal-dielectric photonic crystal in the long wavelength limit. Our results describe the transition between the regime, described by Rytov's formulas for sufficiently long waves, and that predicted by Xu et al. [6], where the effective plasma frequency is independent of the metallic-layer parameters. The derived expressions can be useful for determining the frequency intervals where such an anisotropic system can exhibit metamaterial behavior.

Received 13 February 2011, Accepted 28 March 2011, Scheduled 31 March 2011
Corresponding author: Felipe Perez-Rodriguez (fperez@ifuap.buap.mx).

1. INTRODUCTION

A very simple system for designing metamaterials is the periodic heterostructure (also-known as superlattice or one-dimensional (1D) photonic crystal (PC)) composed of alternating metal and dielectric layers (see, e.g., [1–3]). In the regime of long wavelengths, compared with the PC period a, its optical properties can be described by using an effective permittivity tensor. If the permittivity components are of different sign, such an anisotropic medium can support negative refraction without requiring negative permeability [1–3], unlike double-negative metamaterials. Commonly, the permittivity components are calculated within the effective medium approach originally developed by Rytov [4]. So, if the materials of the superlattice layers are local and isotropic, the permittivity tensor is diagonal with principal values [4]:

$$\varepsilon_x = \varepsilon_y = \varepsilon_m f + \varepsilon_d (1 - f), \tag{1}$$

$$\frac{1}{\varepsilon_z} = \frac{1 - f}{\varepsilon_d} + \frac{f}{\varepsilon_m}. \tag{2}$$

Here, the metal and dielectric layers are characterized by their permittivities, ε_m and ε_d, and thicknesses, d_m and d, respectively; $f = d_m/a$ is the metal filling fraction ($a = d_m + d$), and z denotes the direction perpendicular to the planes of the layers in the superlattice. Formulas (1) and (2) hold in the case of very long waves [4], and have also been obtained by using different homogenization methods (see, for example, [2, 5] and references therein).

Employing the Drude model for the frequency (ω)-dependent dielectric function of the metal (i.e., $\varepsilon_m = \varepsilon_0(1 - \omega_P^2/\omega^2)$, where ω_P is the metal plasma frequency, ε_0 is the vacuum permittivity), the components ε_x and ε_y (1) acquire a similar form:

$$\varepsilon_x = \varepsilon_y = \bar{\varepsilon}\varepsilon_0 \left(1 - \frac{\omega_{P,eff}^2}{\omega^2} \right), \tag{3}$$

with $\bar{\varepsilon} = f + \varepsilon_d(1 - f)/\varepsilon_0$ and an effective plasma frequency

$$\omega_{P,eff} = \omega_P \sqrt{\frac{f}{\bar{\varepsilon}}}. \tag{4}$$

This result turns out to be good enough when the values of the filling fraction are not very small ($f \leq 1$). If $f \ll 1$ and the metal layer thickness is comparable with the skin depth ($d_m \sim c/\omega_P$), the cut-off frequency $\omega_{P,eff}$ is close to the value [6]

$$\omega_{P,eff} = \pi c/nd, \tag{5}$$

where $n = \sqrt{\varepsilon_d/\varepsilon_0}$ is the refraction index of the dielectric. Notice that $\omega_{P,eff}$ in Eq. (5) does not depend on the metal permittivity, like the effective plasma frequency for periodic arrays of very thin metal wires [7]. Although the differences between models (4) and (5) have been analyzed in-depth [6, 8], up to now there are no simple analytic expressions for the permittivity components, which can predict both results as well as the crossover between them. In principle, the two regimes could be described within the effective medium approach proposed by Rytov [4]. However, the calculation of the effective permittivity would require the numerical solution of the exact dispersion equation, especially in the case of electromagnetic modes propagating along the z axis [4] and having a low-frequency gap in their photonic band structure.

In the present work, we will calculate the effective permittivity tensor for a binary metal-dielectric superlattice within the homogenization theory recently developed in the work [9]. This theory has the advantage of providing explicit expressions for the effective parameters of the electromagnetic response. We shall apply it to study the plasma-like behavior of the metal-dielectric heterostructure.

2. THEORETICAL FORMALISM

According to the results, reported in [9], the effective *local* electromagnetic response of a PC, which can be bianisotropic in the most general case, is given by

$$\bar{\bar{\mathbf{A}}}_{eff} = \begin{bmatrix} \overleftrightarrow{\boldsymbol{\varepsilon}}_{eff} & \overleftrightarrow{\boldsymbol{\xi}}_{eff} \\ \overleftrightarrow{\boldsymbol{\zeta}}_{eff} & \overleftrightarrow{\boldsymbol{\mu}}_{eff} \end{bmatrix} \equiv \lim_{k\to 0} \frac{1}{\omega} \left\{ \bar{\bar{\mathbf{D}}}^{-1}(\mathbf{k};0,0) \right\}^{-1}. \tag{6}$$

Here, $\overleftrightarrow{\boldsymbol{\varepsilon}}_{eff}$, $\overleftrightarrow{\boldsymbol{\mu}}_{eff}$, $\overleftrightarrow{\boldsymbol{\xi}}_{eff}$, and $\overleftrightarrow{\boldsymbol{\zeta}}_{eff}$ are, respectively, the effective permittivity, permeability, and crossed magneto-electric tensors, $\mathbf{k}$ is the wave vector, and $\{\dots\}^{-1}$ symbolizes the inverse of the 6×6 matrix block $\bar{\bar{\mathbf{D}}}^{-1}(\mathbf{k};0,0)$, which is obtained from the inverse $\bar{\bar{\mathbf{D}}}^{-1}(\mathbf{k};\mathbf{G},\mathbf{G}')$ of the infinite matrix

$$\bar{\bar{\mathbf{D}}}(\mathbf{k};\mathbf{G},\mathbf{G}') = \begin{bmatrix} \overleftrightarrow{\mathbf{0}} & (\mathbf{k}+\mathbf{G})\times \overleftrightarrow{\mathbf{I}} \\ -(\mathbf{k}+\mathbf{G})\times \overleftrightarrow{\mathbf{I}} & \overleftrightarrow{\mathbf{0}} \end{bmatrix} \delta_{\mathbf{G},\mathbf{G}'} + \omega \bar{\bar{\mathbf{A}}}(\mathbf{G}-\mathbf{G}'), \tag{7}$$

where $\mathbf{G}$, $\mathbf{G}'$ are vectors of the reciprocal lattice of the PC, $\delta_{\mathbf{G},\mathbf{G}'}$ stands for the Kronecker delta, and $\bar{\bar{\mathbf{A}}}(\mathbf{G})$ are the Fourier coefficients

of the 6×6 matrix $\bar{\bar{\mathbf{A}}}(\mathbf{r})$ for the material (bianisotropic) response:

$$\bar{\bar{\mathbf{A}}}(\mathbf{r}) \equiv \begin{bmatrix} \overleftrightarrow{\boldsymbol{\varepsilon}}(\mathbf{r}) & \overleftrightarrow{\boldsymbol{\xi}}(\mathbf{r}) \\ \overleftrightarrow{\boldsymbol{\zeta}}(\mathbf{r}) & \overleftrightarrow{\boldsymbol{\mu}}(\mathbf{r}) \end{bmatrix}. \tag{8}$$

In the case of a binary metal-dielectric superlattice composed of isotropic nonmagnetic materials, the crossed magneto-electric tensors in Eq. (8) are 3×3 zero matrices, whereas the permeability tensor is $\overleftrightarrow{\boldsymbol{\mu}} = \mu_0 \overleftrightarrow{\mathbf{I}}$ (μ_0 is the vacuum permeability). Hence,

$$\bar{\bar{\mathbf{A}}}(G_z - G'_z) = \begin{bmatrix} \varepsilon_d \overleftrightarrow{\mathbf{I}} & \overleftrightarrow{\mathbf{0}} \\ \overleftrightarrow{\mathbf{0}} & \mu_0 \overleftrightarrow{\mathbf{I}} \end{bmatrix} \delta_{G_z, G'_z} + \Delta\bar{\bar{\mathbf{A}}}(G_z - G'_z), \tag{9}$$

where

$$\Delta\bar{\bar{\mathbf{A}}}(G_z - G'_z) = \begin{bmatrix} \Delta\varepsilon \overleftrightarrow{\mathbf{I}} & \overleftrightarrow{\mathbf{0}} \\ \overleftrightarrow{\mathbf{0}} & \overleftrightarrow{\mathbf{0}} \end{bmatrix} F(G_z - G'_z), \tag{10}$$

$\Delta\varepsilon = \varepsilon_m - \varepsilon_d$, and $F(G_z) = f \sin(G_z d_m/2)/(G_z d_m/2)$ is the form factor of the metal layer.

The matrix block $\bar{\bar{\mathbf{D}}}^{-1}(0;0,0)$ is obtained by numerically solving the system of algebraic equations for the block column $\bar{\bar{\mathbf{D}}}^{-1}(0;G_z,0)$ given by

$$\sum_{G'_z} \bar{\bar{\mathbf{D}}}(0;G_z,G'_z)\bar{\bar{\mathbf{D}}}^{-1}(0;G'_z,0) = \bar{\bar{\mathbf{I}}}\delta_{G_z,0}, \tag{11}$$

where $\bar{\bar{\mathbf{I}}}$ is the 6×6 unit matrix. In order to physically interpret our numerical results, we shall also derive a simple expression for the effective permittivity tensor for the considered 1D PC, having thin metallic layers. So, Eq. (11) can be rewritten as

$$\omega\bar{\bar{\mathbf{T}}}^{-1}(G_z) \sum_{G'_z} \Delta\bar{\bar{\mathbf{A}}}(G_z - G'_z)\bar{\bar{\mathbf{D}}}^{-1}(0;G'_z,0) + \bar{\bar{\mathbf{D}}}^{-1}(0;G_z,0)$$

$$= \bar{\bar{\mathbf{T}}}^{-1}(0)\delta_{G_z,0}. \tag{12}$$

Here, $\bar{\bar{\mathbf{T}}}^{-1}(G_z)$ [10] is the inverse of

$$\bar{\bar{\mathbf{T}}}(G_z) \equiv \begin{bmatrix} \omega\varepsilon_b \overleftrightarrow{\mathbf{I}} & G_z\hat{z}\times \overleftrightarrow{\mathbf{I}} \\ -G_z\hat{z}\times \overleftrightarrow{\mathbf{I}} & \omega\mu_0 \overleftrightarrow{\mathbf{I}} \end{bmatrix}. \tag{13}$$

Multiplying Eq. (12) by $\Delta\bar{\bar{\mathbf{A}}}(-G_z)$ and summing over G_z, we get

$$\omega \sum_{G_z} \Delta\bar{\bar{\mathbf{A}}}(-G_z)\bar{\bar{\mathbf{T}}}^{-1}(G_z) \sum_{G'_z} \Delta\bar{\bar{\mathbf{A}}}(G_z - G'_z)\bar{\bar{\mathbf{D}}}^{-1}(0;G'_z,0)$$

$$+ \sum_{G_z} \Delta\bar{\bar{\mathbf{A}}}(-G_z)\bar{\bar{\mathbf{D}}}^{-1}(0;G_z,0) = \Delta\bar{\bar{\mathbf{A}}}(0)\bar{\bar{\mathbf{T}}}^{-1}(0). \tag{14}$$

It can be shown that in the case $fk_d a \ll 1$ (i.e., $k_d d_m \ll 1$), where $k_d = n\omega/c$, the relation

$$\sum_{G_z} \Delta\bar{\bar{\mathbf{A}}}(-G_z)\bar{\bar{\mathbf{T}}}^{-1}(G_z)\Delta\bar{\bar{\mathbf{A}}}(G_z - G'_z) \approx \begin{bmatrix} \overleftrightarrow{\mathbf{S}} & \overleftrightarrow{\mathbf{0}} \\ \overleftrightarrow{\mathbf{0}} & \overleftrightarrow{\mathbf{0}} \end{bmatrix} \begin{bmatrix} \Delta\varepsilon\,\overleftrightarrow{\mathbf{I}} & \overleftrightarrow{\mathbf{0}} \\ \overleftrightarrow{\mathbf{0}} & \overleftrightarrow{\mathbf{0}} \end{bmatrix} F(-G'_z), \tag{15}$$

with $(\overleftrightarrow{\mathbf{S}})_{ij} = S_i\delta_{ij}$ [$S_x = S_y = \Delta\varepsilon\, d_m\sqrt{\mu_0}/(2\sqrt{\varepsilon_d}\tan(k_d a))$, $S_z = \Delta\varepsilon/(\omega\varepsilon_d)$], is asymptotically correct. Using this relation in Eq. (14), we get

$$\sum_{G_z} \Delta\bar{\bar{\mathbf{A}}}(-G_z)\bar{\bar{\mathbf{D}}}^{-1}(0;G_z,0) = \left[\bar{\bar{\mathbf{I}}} + \omega\begin{bmatrix} \overleftrightarrow{\mathbf{S}} & \overleftrightarrow{\mathbf{0}} \\ \overleftrightarrow{\mathbf{0}} & \overleftrightarrow{\mathbf{0}} \end{bmatrix}\right]^{-1} \Delta\bar{\bar{\mathbf{A}}}(0)\bar{\bar{\mathbf{T}}}^{-1}(0). \tag{16}$$

After substituting the sum (16) into (12) for $G_z = 0$, we obtain an analytical expression for the matrix block $\bar{\bar{\mathbf{D}}}^{-1}(0;0,0)$, whose 6×6 inverse matrix determines $\bar{\bar{\mathbf{A}}}_{eff}$ (Eq. (6)), having submatrices: $\varepsilon_{eff,ij} = \varepsilon_i\delta_{ij}$, $\mu_{eff,ij} = \mu_0\delta_{ij}$, and $\xi_{eff,ij} = \zeta_{eff,ij} = 0$. The components ε_x and ε_y of the effective permittivity can be expressed as

$$\varepsilon_x = \varepsilon_y = \varepsilon_d\left(1 - \frac{1}{1 - \frac{(\omega a/2c)\sqrt{\varepsilon_d/\varepsilon_0}}{\tan\left[(\omega a/2c)\sqrt{\varepsilon_d/\varepsilon_0}\right]} - \frac{\varepsilon_d}{f(\varepsilon_m - \varepsilon_d)}}\right), \tag{17}$$

whereas our result for the component ε_z goes over into formula (2). Besides, in deriving ε_z the condition $k_d d_m \ll 1$ was not needed, unlike the analytical calculation of $\varepsilon_x = \varepsilon_y$ (17).

Notice that Rytov expression (1) for ε_x and ε_y is obtained from Eq. (17) in the limit $k_d a \to 0$ as well as in the case of small metal filling fraction ($f \ll 1$) and moderate dielectric contrast (i.e., $\varepsilon_d/f|\varepsilon_m - \varepsilon_d| \gg 1$). However, as we will show below, at sufficiently-large dielectric contrast, namely at $d_m \sim c/\omega_P \ll d$ (i.e., $\varepsilon_d/f|\varepsilon_m - \varepsilon_d| \sim (\omega/\omega_P)(\omega d/c) \ll 1$), our formula (17) tends to the permittivity (3) with the effective plasma frequency (5) proposed by Xu et al. [6].

3. DISCUSSION

Using Eqs. (6), (7), and (9), we have numerically calculated the 6×6 matrix $\bar{\bar{\mathbf{A}}}_{eff}$ of the effective local electromagnetic response for

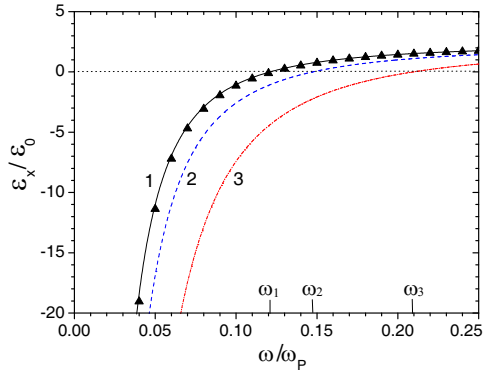

Figure 1. Frequency dependence of the effective permittivity ε_x for a metal-dielectric superlattice with $d_m = 0.5c/\omega_P$, $d = 10c/\omega_P$, and $n = 1.5$. The triangles and curve 1 were obtained by using Eqs. (6) and (17), respectively. For calculating curve 2 [curve 3], we used the model (3) with Eq. (4) [Eq. (5)]. ω_1, ω_2, and ω_3 indicate the zeros of $\varepsilon_x(\omega)$ corresponding to curves 1, 2, and 3.

a supperlattice with $d_m = 0.5c/\omega_P$, $d = 10c/\omega_P$ and $\varepsilon_d = 2.25\varepsilon_0$ ($n = 1.5$) as that considered in [6]. Fig. 1 exhibits our numerical results for the frequency dependence of the permittivity component ε_x ($= \varepsilon_y$) [see triangles therein]. Evidently, the predictions of the formula (17) (solid line, labeled with number 1 in Fig. 1) coincide with the numerical results. Notice that $\varepsilon_x(\omega)$ has a zero at $\omega = \omega_1 \approx 0.121\omega_P$, which indicates the top or width of the low-frequency band gap ($0 < \omega < \omega_1$) in the photonic band structure for modes propagating along the growth direction of the metal-dielectric superlattice (Fig. 2). Interestingly, the dispersion relation $k(\omega) = (\omega/c)\sqrt{\varepsilon_x/\varepsilon_0}$, calculated with the effective permittivity (17), describes not only the low-frequency band gap, but also the lowest pass band for photonic modes up to the middle ($ka/\pi \sim 0.5$) of the first Brillouin zone (see Fig. 2). We have also calculated the effective permittivity $\varepsilon_x(\omega)$, given by Eq. (3), using the cut-off frequencies (4) and (5) (see curves 2 and 3 in Fig. 1). As is seen, the effective plasma frequencies $\omega_2 = 0.147\omega_P$ and $\omega_3 = 0.209\omega_P$, predicted by such models, are larger than the exact result.

Figure 3 presents the dependencies of $1/\omega_{P,eff}$ (panel "a") and $\omega_{P,eff}$ (panel "b") upon the parameter $\omega_P nd/c$, which were calculated with the models (17) (curve 1), (4) (curve 2), and (5) (curve 3). At small values of $\omega_P nd/c$, our results (curve 1) agree with Rytov's formula (curve 2) so that $\omega_P/\omega_{P,eff}$ approaches one as $\omega_P nd/c \to 0$. This result is physically clear because the superlattice converts into

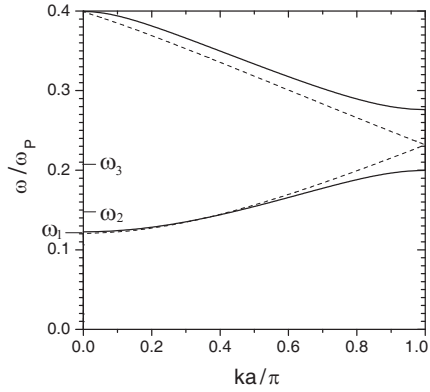

Figure 2. Solid line: photonic band structure for a metal-dielectric superlattice as in Fig. 1. Dashed line: dispersion relation obtained by using the effective permittivity $\varepsilon_x(\omega)$ (curve 1) from Fig. 1.

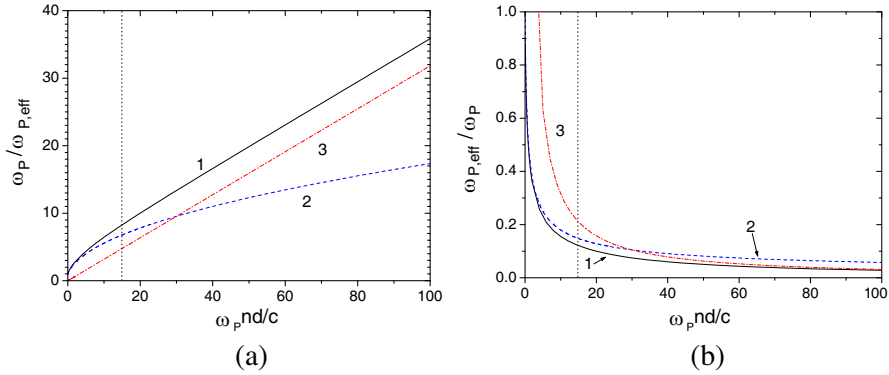

Figure 3. Dependence of (a) $1/\omega_{P,eff}$ and (b) $\omega_{P,eff}$ on the parameter $\omega_P nd/c$ for a metal-dielectric superlattice with $d_m = 0.5c/\omega_P$. Curves 1, 2 and 3 were calculated by using Eqs. (17), (4), and (5), respectively.

a homogeneous metallic medium with $\omega_{P,eff} = \omega_P$ if $d \to 0$. On the other hand, at large values of $\omega_P nd/c$, the curves 1 and 3 in Fig. 3(a) become parallel straight lines, and Rytov's result considerably differs from our curve 1, which coincides with the reciprocal value of the cut-off frequency obtained from the exact photonic band structure. The slope of line 3 allowed Xu *et al.* to determine $\omega_{P,eff}$ (5) (see Fig. 2 in [6]) with sufficiently accuracy. Indeed, the constant difference between our result for $1/\omega_{P,eff}$ and the straight line 3 in Fig. 3, is negligible for the reciprocal function, namely $\omega_{P,eff}$, at $\omega_P nd/c \gg 1$. Therefore,

the curves 1 and 3 in the panel "b" approach each other as $\omega_P nd/c$ increases. The dotted vertical line in both panels of Fig. 3 indicates the value of the parameter $\omega_P nd/c = 15$ which was used for calculating the graphs in Figs. 1 and 2 (and Fig. 1 in [6]). As is seen in Fig. 3(b), the value $\omega_P nd/c = 15$ is in a relatively-broad interval where neither formula (4) nor (5) predicts correct values for $\omega_{P,eff}$.

In Figs. 4 and 5, we show the frequency-dependence of the effective permittivity ε_x and the photonic dispersion for a superlattice with the same parameters as in Fig. 1, except that $d = 100c/\omega_P$. Fig. 4 demonstrates the excellent agreement between analytical (curve 1) and numerical (triangles) results. It is evident that in this case the predictions by Xu et al. (Eqs. (3) and (5)) are very close to our calculations of permittivity $\varepsilon_x(\omega)$ (compare curves 1 and 3 in Fig. 4. In Fig. 5, one can observe that the effective plasma frequency $\omega_1 = 0.0193\omega_P$, predicted by model (17), completely agrees with the band structure calculations and is close to $\omega_3 = 0.0209\omega_P$ given by Eq. (5). However, ω_2 (4), obtained from Rytov's formula (1), has a larger value ($\omega_2 = 0.047\omega_P$), being above the second pass band. The large difference between ω_2 and the width of the low-frequency band gap (see Fig. 5) is owing to the fact that in a metal with thickness d_m of the order of the skin depth ($d_m \sim c/\omega_P \ll d$) the condition of slight variation of the "microfield" across the metal layer, which was used in [4] in deriving formula (1), is not satisfied.

It should be commented that we have neglected damping effects,

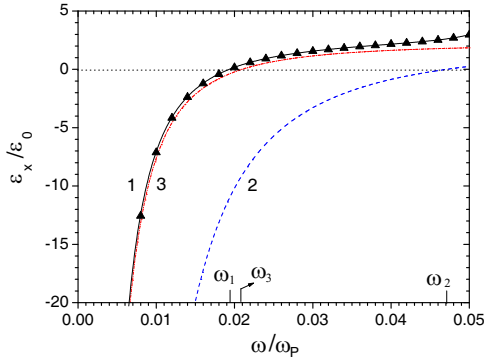

Figure 4. Frequency dependence of the effective permittivity ε_x for a metal-dielectric superlattice with $d_m = 0.5c/\omega_P$, $d = 100c/\omega_P$, and $n = 1.5$. The triangles and curve 1 were obtained by using Eqs. (6) and (17), respectively. For calculating curve 2 [curve 3], we used the model (3) with Eq. (4) [Eq. (5)]. ω_1, ω_2, and ω_3 indicate the zeros of $\varepsilon_x(\omega)$ corresponding to curves 1, 2, and 3.

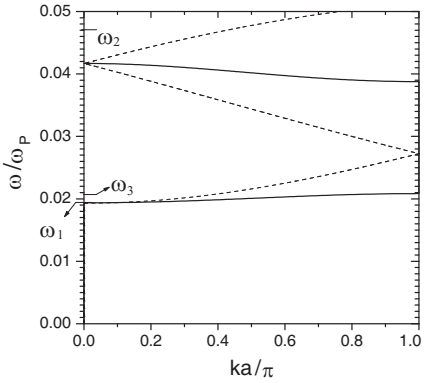

Figure 5. Solid line: Photonic band structure for a metal-dielectric superlattice as in Fig. 4. Dashed line: Dispersion relation obtained by using the effective permittivity $\varepsilon_x(\omega)$ [Eq. (17)].

which can be included in the Drude model by introducing a relaxation frequency ν, typically ranging in the THz region, as: $\varepsilon_m = \varepsilon_0(1 - \omega_P^2/(\omega^2 + i\omega\nu))$. Hence, the cut-off frequency will be well defined at frequencies $\omega \gg \nu$, where losses in the metal inclusion are small. Drude model is commonly used for bulk metal samples. However, this local model also describes the electromagnetic response of thin metal films ($d_m \sim c/\omega_P$) in the optical range, since the effects of spatial dispersion manifest themselves at much lower frequencies, namely in the THz region (see [11]).

4. CONCLUSION

In this work, we have applied the homogenization theory developed in [9] to calculate the frequency-dependent effective *local* permittivity tensor of a metal-dielectric superlattice. We could also derive analytic expressions for the components of the permittivity tensor, describing both the regime, where Rytov's formulas [4] are valid, and that found by Xu et al. [6] at very small metal filling fractions. Our results could be useful in designing metamaterials based on metal-dielectric 1D PC.

ACKNOWLEDGMENT

This work was partially supported by CONACYT (through Red Temática de Nanociencia y Nanotecnología) and VIEP-BUAP (grants MAN-ING10-G and 50-EXC10-I).

REFERENCES

1. Podolskiy, V. A. and E. E. Narimanov, "Strongly anisotropic waveguide as a nonmagnetic left-handed system," *Phys. Rev. B*, Vol. 71, 201101(R), 1–4, 2005.
2. Wood, B., J. B. Pendry, and D. P. Tsai, "Directed subwavelength imaging using a layered metal-dielectric system," *Phys. Rev. B*, Vol. 74, 115116, 1–8, 2006.
3. Rakhmanov, A. L., V. A. Yampolskii, J. A. Fan, F. Capasso, and F. Nori, "Layered superconductors as negative-refractive-index metamaterials," *Phys. Rev. B*, Vol. 81, 075101, 1–6, 2010.
4. Rytov, S. M., "Electromagnetic properties of a finely stratified medium," *Sov. Phys. JETP*, Vol. 2, 466–475, 1956.
5. Bergman, D. J. and D. Stroud, "Physical properties of macroscopically inhomogeneous media," *Solid State Phys.*, Vol. 46, 147–269, 1992.
6. Xu, X., Y. Xi, D. Han, X. Liu, J. Zi, and Z. Zhu, "Effective plasma frequency in one-dimensional metallic-dielectric photonic crystals," *Appl. Phys. Lett.*, Vol. 86, 091112, 1–3, 2005.
7. Pendry, J. B., A. J. Holden, W. J. Stewart, and I. Youngs, "Extremely low frequency plasmons in metallic mesostructures," *Phys. Rev. Lett.*, Vol. 76, 4773–4776, 1996.
8. Manzanarez-Martínez, J., "Analytic expression for the effective plasma frequency in one-dimensional metallic-dielectric photonic crystal," *Progress In Electromagnetics Research M*, Vol. 13, 189–202, 2010.
9. Cerdán-Ramírez, V., B. Zenteno-Mateo, M. P. Sampedro, M. A. Palomino-Ovando, B. Flores-Desirena, and F. Pérez-Rodríguez, "Anisotropy effects in homogenized magnetodielectric photonic crystals," *J. Appl. Phys.*, Vol. 106, 103520, 1–8, 2009.
10. An explicit expression for $\bar{\bar{\mathbf{T}}}^{-1}(\mathbf{G})$ has been derived in Ref. [9] (see Eqs. (33)–(37) therein).
11. Paredes-Juárez, A., F. Días-Monge, N. M. Makarov, and F. Pérez-Rodríguez, "Nonlocal effects in the electrodynamics of metallic slabs," *JETP Lett.*, Vol. 90, 623–627, 2009.